Biomaterials 33 (2012) 2345–2350

Contents lists available at SciVerse ScienceDirect

Biomaterials

journal homepage: www.elsevier.com/locate/biomaterials

Off-resonance plasmonic enhanced femtosecond laser optoporation and transfection of cancer cells

Judith Baumgart [a], Laure Humbert [b], Étienne Boulais [a], Rémi Lachaine [a], Jean-Jaques Lebrun [b], Michel Meunier [a,*]

[a] École Polytechnique de Montréal, Laser Processing and Plasmonics Laboratory, Engineering Physics Department, Montréal, Québec H3C 3A7, Canada
[b] Royal Victoria Hospital, Department of Medicine, Montréal, Québec H3A 1A1, Canada

ARTICLE INFO

Article history:
Received 3 November 2011
Accepted 22 November 2011
Available online 15 December 2011

Keywords:
Optoperforation
Transfection
Gold nanoparticle
Plasmonic
Femtosecond laser
Cancer cell

ABSTRACT

A femtosecond laser based transfection method using off-resonance plasmonic gold nanoparticles is described. For human cancer melanoma cells, the treatment leads to a very high perforation rate of 70%, transfection efficiency three times higher than for conventional lipofection, and very low toxicity (<1%). Off-resonance laser excitation inhibited the fracture of the nanoparticles into possibly toxic DNA intercalating particles. This efficient and low toxicity method is a promising alternative to viral transfection for skin cancer treatment.

1. Introduction

Transfection is a method widely used by biologists for transferring foreign genetic material into mammalian cells. None of the current techniques, including transfection via viral carriers [1], electroporation [2–4], or liposomes [5–8], is entirely satisfactory and for each method efficiency strongly depends on the cell type and/or the vector used to deliver the gene of interest. More importantly, delivering genetic foreign material to target cells with high efficiency in vivo remains extremely challenging and represents a limitation of current gene therapy approaches [9–11]. Even if techniques relying on the use of viral-mediated gene delivery show superior gene transfer efficacy, they also face major safety and immunogenicity concerns. Other non-viral methods have thus become attractive alternatives for human gene therapy. Human DNA is less expensive, easy to produce, has negligible immunogenicity, and raises less safety concerns compared to viral vectors preparation. However, the transfection of this naked DNA by current available methods shows major disadvantages, including a low level of transfection efficiency in vivo, lack of sustained expression, as well as tissue damage. Therefore, technical improvements in transfection methodology are required before non-viral gene therapy can successfully be used as therapeutic tools in the clinic.

Single cells of many different types including stem and primary cells have already been transfected with high perforation efficiency and with very low cell damage using a tightly focused fs laser [12–17]. However this technique is limited to a very low throughput and thus is inappropriate for most biological or medical applications, which most often require a high population of transfected cells. Permeabilization of cell membrane using nanosecond pulsed laser resonant gold nanoparticles has also been reported [18–20]. However, because the basic mechanisms [21–23] rely on the extreme heating of the nanostructures, major cytotoxicity concerns are raised by the possible particle fragmentation. In this paper, we present a fs laser high throughput virus-free and fragmentation-free transfection method based on the dispersion of out of resonant spherical gold nanoparticles (AuNP) on the cells, followed by an irradiation using a low fluence from a weakly focused fs laser. Low fluence is defined by a resulting irradiance on the cells ($I = 2 \times 10^{12}$ W/cm^2 in our case) well below the optical breakdown condition ($I_{\text{breakdown}} \sim 1 \times 10^{13}$ W/cm^2 for 45 fs pulse [22]), thus preventing any laser-induced optoperforation without the presence of nanoparticles.

The feasibility of this method has been shown earlier in a preliminary study by Schomaker et al. [24] without presenting any detailed data about toxicity, long term viability of the treated cells, transfection efficiency, statistically relevant numbers of

* Corresponding author.
E-mail address: michel.meunier@polymtl.ca (M. Meunier).

0142-9612/$ – see front matter © 2011 Elsevier Ltd. All rights reserved.
doi:10.1016/j.biomaterials.2011.11.062

transfected cells, process description or comparison with existing transfection methods. This paper presents a complete characterization of the technique when applied to the transfection of human cancer melanoma cells, which presents very interesting perspectives for this kind of optical transfection process. Indeed, over the past 50 years, the incidence of melanoma in most developed countries has increased faster than any other cancer and melanoma is now the most common cause of cancer deaths in young adults between the ages 20–35 [25]. While melanoma accounts for only 5% of skin cancers, it is responsible for 80% of all skin cancer deaths. Although most patients have localized disease at the time of diagnosis and are cured by surgical excision of the primary tumour, melanoma can be highly malignant, and form metastases to almost any organ of the body, leading to the death of the patient. There is thus an urgent need for the development of novel therapies to fight this disease. The skin is an attractive model tissue for gene delivery using fs laser gene transfer. Indeed, as the tissue is exposed to the outside of the organism, this could allow for non-invasive introduction of foreign DNA using an articulated fs mobile laser, following intradermal injection of the nanoparticles and DNA material. In such case, the gene transfer could be precisely directed towards chosen cell layers within the skin by determining specific irradiated areas and depth at the site of injection. Thus, one could implement this technique to clinical setup and use this gene transfection method to efficiently deliver cell damaging or cytotoxic DNA into dysplastic cells such as melanoma cells to block tumour formation and prevent the progression of the disease to metastatic stages.

2. Material and methods

2.1. Sample preparation and laser treatment

The cells were incubated during 3–6 h with the AuNP (8 μg/ml, diameter 100 nm, Nanopartz) in the culture medium at 37 °C and 5% CO_2 and then washed once with PBS. Afterwards, fresh medium was added to the dishes including the molecules that were meant to be introduced to the cells by the laser treatment: LY (Lucifer Yellow, Invitrogen), YFP-SMAD2 plasmid [26].

The laser treatment was performed by using a femtosecond laser (Spitfire, Spectra Physics) at a central wavelength of 800 nm, a repetition rate of 1 kHz, and maximum output pulse energy of 5 mJ. The laser beam was attenuated by a Brewster window and a polarizer and guided through a focussing plano-convex lens ($f = 75$ mm) to the sample. The sample was irradiated from below with a Gaussian beam profile and a spot size of 650 μm in diameter through the glass slide of the glass bottom dishes. A three axis scanning table performed the movement of the sample to irradiate the whole or parts of the glass bottom of the petri dish with a scanning velocity of 3.5 mm/s and a line to line step-size of 280 μm. The treatment of the complete petri dish (314 mm^2) took about 8 min.

After the laser treatment, the cells were washed twice or once to remove the LY or the DNA respectively. For transfection, the cells were observed by fluorescence microscopy 48 h after the treatment. Cell counting was performed automatically by software (Image Pro Plus, Media Cybernetics Inc.), taking into account the brightness of fluorescent cells of the respective fluorescent dyes. During all perforation and laser transfection experiments at least $2.2x10^3$ cells were treated per experiment at a confluence of 80%. Negative control (nanoparticles present but no laser irradiation) was performed at the same time in the same culture dish, about 1.5×10^5 cells per experiment. Additional negative control (laser irradiation at optimum fluence for nanoparticle-enhanced laser perforation but no nanoparticles present) was performed independently.

2.2. Transfection by lipofection

Transfection of WM278 cells by lipofection was performed using Lipofectamine 2000 reagent (Invitrogen) in the conditions previously optimized in the laboratory. Briefly, 2 μg plasmid was mixed with 10 μl Lipofectamine 2000 reagent and Optimem media (Invitrogen) and added to WM278 cells in glass bottom dishes (MatTek Corp.). Cells were then incubated at 37 °C in a 5% CO_2 incubator. About 2×10^5 cells were treated per experiment.

2.3. Perforation rate and viability by fluorescence microscopy

The perforation rate was estimated by measuring the uptake of LY, which was present in the medium during the laser treatment. Two hours after the treatment, 1.5 μM PI (Propidium Iodide, Sigma Aldrich) were added to the cell medium for 10 min, then washed once. Afterwards, the cells were fixed incubating the cells in 3.7% Formaldehyde (Sigma Aldrich) and PBS for 10 min, washed once, then added 10 μM DAPI (4′,6-Diamidino-2-phenylindole dihydrochloride, Sigma Aldrich) for 10 min and washed once. The cells were then stored at 4 °C.

2.4. Cell culture

WM278 human melanoma cells were cultured in RPMI 1640 (Gibco) containing 10% FBS (Gibco) supplemented with penicillin-streptomycin (Fisher Scientific) and L-Glutamine (2 mM) (Fisher Scientific). They were incubated at 37 °C and 5% CO_2 atmosphere. The cells were trypsinized and seeded onto glass bottom dishes ($1x10^5$ cells, MatTek Corp.) about 24 h before the laser treatment.

2.5. Perforation rate and viability by fluorescence microscopy

Observation of perforation rate (LY, green fluorescence) and viability (PI, red fluorescence) was performed using an inverted fluorescence microscope (Axio Observer, Colibri illumination system, Zeiss). The viability was calculated by $V = 1-N_{PI}/N_{DAPI}$, the perforation rate by $P = (N_{LY}-N_{PI})/N_{DAPI}$, so that only viable perforated cells were counted. At high fluences, the total number of present cells (DAPI, blue fluorescence) had to be corrected as many cells were detached due to the laser irradiation and the confluence of the cells in the irradiated areas was lower than in the control areas (non-irradiated areas in the same petri dish). This difference was added to the total number of cells N_{DAPI} as well as to the number of dead cells N_{PI}. Cell counting was performed as for the transfected cells (see section Laser treatment).

2.6. Toxicity of nanoparticules by MTT assay and long term viability after laser treatment

The cytotoxicity of the AuNP was measured by performing an MTT assay (3-(4,5-Dimethylthiazol-2-yl)-2,5-diphenyltetrazolium bromide, TOX1, Sigma Aldrich). $3.5x10^3$ cells per well were plated into a 96-well plate, 24 h before adding the AuNP (concentration: 15 and 75 μg/ml). The cells were incubated in the culture medium with AuNP during 3, 6, and 12 h and then washed with PBS once. Afterwards, the cells were incubated in the culture medium for 36 h. Then, the absorption of the AuNP in the cells at 570 nm was measured using a plate reader, before adding the MTT reagent for 2 h, before adding the solvent (acidic isopropanol) to dilute the formed crystals. 24 h later, the absorption was measured at 570 nm again. The difference of the absorption A_{NP} of the first and A_{all} of the second measurement gave the total absorption of the MTT reagent $A_{MTT} = A_{all}-A_{NP}$ and therefore the proliferation of the cells during the 36 h.

The same procedure was performed after the laser treatment to measure the long term viability of the cells after the laser treatment. In this case, the AuNP were incubated during 6 h before the treatment. The MTT assay was performed 2, 24, 48, and 72 h after the treatment.

The cytotoxicity of the transfection by lipofection was measured by performing an MTT assay (3-(4,5-Dimethylthiazol-2-yl)-2,5-diphenyltetrazolium bromide, Sigma Aldrich) 2 h–72 h post-transfection. Briefly, 5×10^3 WM278 cells were seeded in 96-well plates and transfected following the optimized transfection conditions, as well as with 2 times more lipofectamine. 25 μl MTT (5 mg ml^{-1} in PBS) was added to the medium and cells were incubated for 2 h at 37 °C in a 5% CO_2 incubator. 100 μl of a 50% H_2O 50% dimethylformamide 20% SDS pH 4.7 solution was added. The absorbance was measured at 570 nm with a reference wavelength at 690 nm. The Optimem transfection medium was exchanged 8 h after the transfection by culture medium (2% FBS).

2.7. SEM imaging

The imaging of the cells and the AuNP was performed using a SEM (Scanning Electron Microscope, Quanta, FEI) in low vacuum mode. The cells were fixed in 5% Glutaraldehyde in PBS for 30 min, then in 5% Glutaraldehyde in water for 30 min. The cells were dried before putting them into the vacuum chamber of the SEM.

2.8. In-situ spectroscopy

The same laser setup and nanoparticles as in the transfection experiment were used to make in-situ spectroscopic measurements. A four faces polished cuvette was filled with the nanoparticle solution in which Dextran (Leuconostoc ssp. Mr ~ 40,000) was added with concentration of 1 mg/ml to reduce aggregation. A white light source (StellarNet SL1, 400–900 nm) probed the sample perpendicularly to the femtosecond laser beam and the absorption spectra were acquired at every minute for a total of 12 h by using a spectrometer (Ocean Optics USB4000).

2.9. Confocal microscopy

The imaging of the AuNP inside the cells was performed using a confocal microscope (FV1000, Olympus). A 60× oil objective with a numerical aperture of

1.42 was used to focus the laser into the sample. The laser wavelengths used were 488 nm for the AuNP and 543 nm for the FM 4–64 FX membrane dye.

3. Results and discussion

3.1. Specificity of the off-resonance plasmonic enhanced laser-induced cell membrane perforation mechanism

Fs laser-induced transfection is usually associated with the production of a cavitation bubble near the cell membrane, and the same mechanism is expected in the case of plasmonic enhanced laser-induced transfection [13,14,23]. Fs laser interaction with off-resonance nanoparticles creates small nanoscale pores in the membrane based on the local electric field amplification of the incident laser. Indeed, even for off-resonance plasmonic nanostructures, a near field amplification occurs upon irradiation (~4.5X for a 100 nm AuNPs irradiated at 800 nm) resulting in an irradiance way above the optical breakdown threshold ($(4.5)^2 \times I > I_{breakdown}$ where I is 2×10^{12} W/cm^2 in our case and $I_{breakdown} \sim 1 \times 10^{13}$ W/cm^2 for 45 fs pulse [22]). This produces a highly localized plasma in the biological media surrounding the nanoparticles that relaxes rapidly (~100 fs-1 ps) through electron–ion interaction, leading eventually to a localized phase transformation and cavitation bubble. Small absorption of the off-resonance nanoparticles results in its temperature increase and to a slow (~1–10 ps) water heating process, but this proves to be insufficient to produce a cavitation bubble under effective transfection fluences (~100 mJ/cm^2). The cavitation bubble thus comes from the relaxation of the plasma and not from the particle heating. This result is supported by calculations performed using a complete model including description of the nanoparticle heating, plasma and water dynamic as well as thermodynamic state evolution that demonstrate that for the laser parameters used in our transfection experiments, energy transfer from the nanoparticle alone cannot explain the generation of a cavitation bubble, whereas the addition of plasma relaxation creates a sub-micrometric cavitation bubble. More details about the model will be published elsewhere. In summary, the use of off-resonance spherical gold nanoparticles allows to reduce the energy absorption by the nanoparticle, inhibiting its fragmentation, while using the scattered field to produce a plasma which induces the nanocavitation process responsible for the cell membrane permeabilization.

In particular, this approach is very different from the carbon nanoparticle-enhanced fs laser optoporation of cells recently proposed by Chakraverty et al. [27]. Their approach was based on the transient permeabilization of the cell membrane by photoacoustic forces resulting from thermally induced decomposition of strongly absorbing 25 nm carbon black agglomerated nanoparticles. The proposed process is different here as the 100 nm AuNPs do not significantly absorb photon energy but rather amplify the scattered near field [28] to induce in the biological media a highly localized electronic plasma and bubbles (optical breakdown) leading to cell optoporation [14,23].

3.2. Nanoparticle localization and cytotoxicity

In nanoparticle-enhanced fs laser transfection, the localization of the nanoparticles will have a significant effect on the transfection efficiency and viability of the cell following the laser irradiation. While the nanoparticles located near the cell membrane contribute significantly to its overall permeabilization, the AuNP internalization might affect the cell viability. Fig. 1 shows cytotoxicity results and confocal microscopy and scanning electron microscopy (SEM) images to localize the nanoparticles. The SEM images (Fig. 1a) taken after an incubation time of 6 h with a AuNP concentration of 8 μg/ml show that the distribution of AuNP at the membrane outside the cell are more likely located near the nucleus. In average, for an incubation concentration of 8 μg/ml of AuNP, approximately 90 ± 23 AuNP per cell were counted. Furthermore, confocal images indeed revealed that a fraction of the AuNP were internalized (Fig. 1c). However, the actual ratio could not be found due to the limiting spatial resolution of the measurement.

General cytotoxicity of bare AuNP has therefore been assessed in order to ensure that cells are not adversely affected by their internalisation prior to the treatment. The cytotoxicity was measured by cell viability MTT assay on a human cancer cell line (WM278) originated from a patient with melanoma, isolated at the Wistar Institute [29]. In the conditions used for transfection (see below), the gold nanostructures show very low toxicity of less than 1%. However, at a 1.9× and 9.4× concentrations, the toxicity was found to be dependent on the co-incubation time of the cells with 100 nm spherical AuNP (see Fig. 1d). At a AuNP concentration of 15 μg/ml (1.9×), the viability of the cells measured after 36 h was 100%, 99.5% and 91.2% for an incubation time of 3 h, 6 h, and 12 h, respectively. By increasing the concentration to 75 μg/ml (9.4×), the viability of the cells was slightly lower at 99.5%, 98.2%, and 91.1% after an incubation time with the particles of 3 h, 6 h, and 12 h, respectively. In both cases, the large drop of the cell viability after 12 h of incubation could be related to an increase of the total number of AuNP per cell resulting from their strong sedimentation and sets the upper limit for the incubation time.

3.3. Perforation rate and long term viability in comparison to lipofection

Irradiation of NPs located at the cell membrane will open nanoscale pores allowing extracellular material to enter the cell. To demonstrate this, we performed laser optoporation in vitro to introduce the fluorescent dye Lucifer Yellow (LY) or DNA plasmids. LY was used as a proof of an uptake of extracellular molecules due to the plasmonic enhanced fs laser pulses as this dye cannot penetrate through the intact cellular membrane. The plasmonic enhanced laser treatment leads to a very high perforation rate of up to 70% at a viability of 80% of the treated cells including the 1% cytotoxicity of the AuNP (see Fig. 2a and b). The maximum perforation rate was achieved for a fluence of 100–120 mJ/cm^2. At higher fluences, the viability of the WM278 cells decreases to only 10% whereas it was constant at about 80% for fluences from 60 to 120 mJ/cm^2. Hence, under rather weak laser irradiation, both internalized nanoparticles and nanoparticles at the cell membrane have a very small effect on the short term cell viability. Negative controls showed that there was no uptake of fluorescent molecules (or DNA) into cells loaded with nanoparticles when not irradiatied (<0. 1%). Similarly, irradiated cells without nanoparticles at a fluence of 100 mJ/cm^2 resulted also in no uptake (<0. 1%). A very high selectivity is therefore reached as only nanoparticle loaded cells that are irradiated are perforated.

The long term viability of the cells after the laser treatment was also measured using MTT assay. The viability of the cells was measured 2 h, 24 h, 48 h, and 72 h after the laser treatment, which was performed at 100 mJ/cm^2 and at the same scanning conditions as the perforation experiments. The cells were incubated with 8 μg/ml spherical AuNP of a diameter of 100 nm during 4 h–6 h before the laser treatment. The 80% viability 2 h after treatment is in very good agreement with the viability measurement using Propidium Iodide (PI) as marker shown in Fig. 2a. During 24 h–72 h after the laser treatment, the viability increases slightly to 87%, 90%, and 95%, respectively. This increase is explained by the proliferation of the cells in the culture medium containing 2% fetal bovine serum (FBS), and indicates that the cell membrane recovers after the

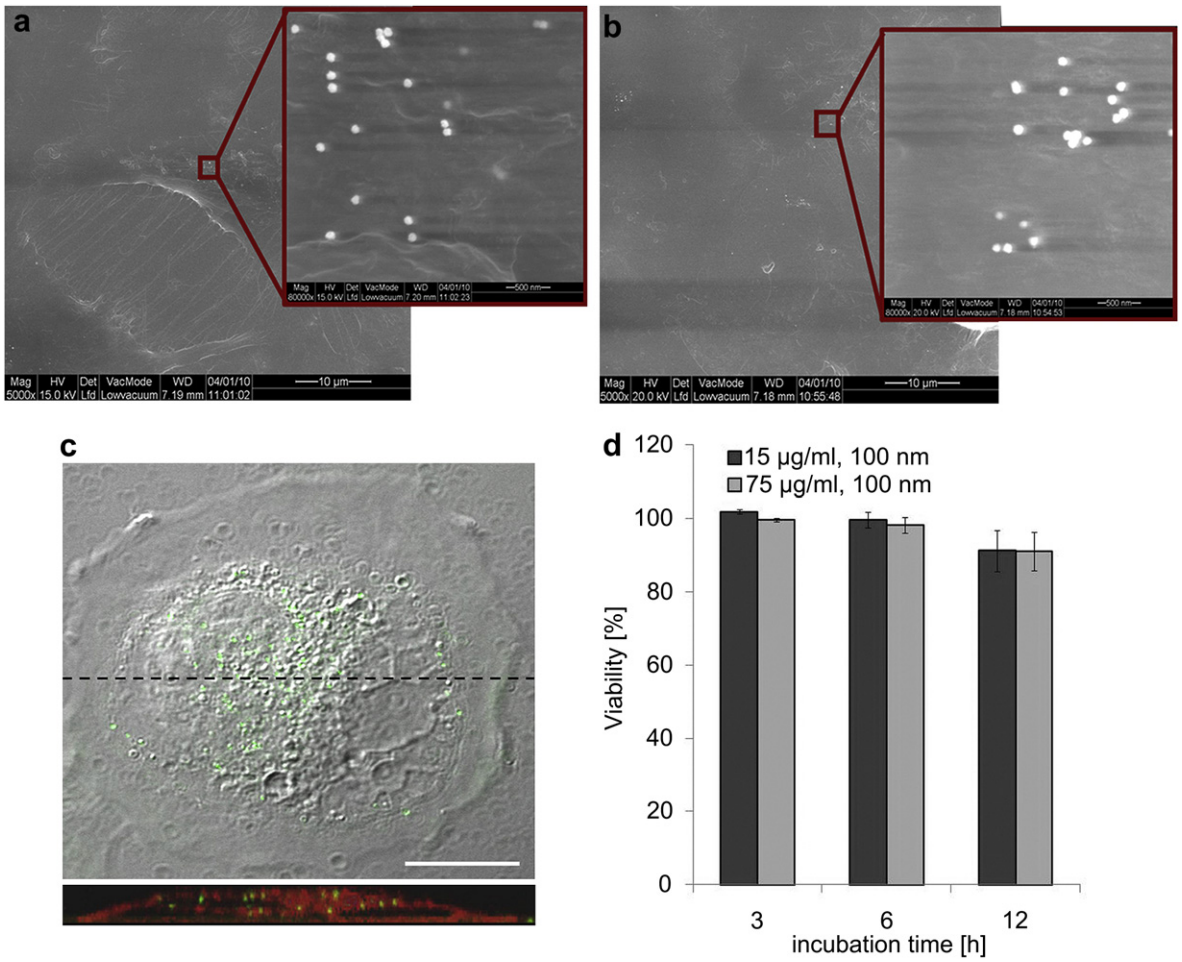

Fig. 1. Cytotoxicity and localization of the AuNP. (a) SEM images (low vacuum mode) of human melanoma cells and spherical AuNP (ø = 100 nm) on the cell membrane without laser treatment and (b) after laser treatment at a fluence of 100 mJ/cm^2. Scale bars: 10 µm, in zoom in images: 100 nm. (c) Confocal microscopy images of human melanoma cells showing the AuNP inside the cells after an incubation time of 6 h. Top: the image was taken at a distance of 1.5 µm to the glass slide; bottom: the confocal fluorescence image of the cross section through the cell (dashed line). The green fluorescence represents scattering light of the AuNP, the red fluorescence was emitted by the membrane dye FM 4–64 FX. The thickness of the cross section is 9 µm. Scale bar: 10 µm. (d) Human melanoma cells were incubated with AuNP (ø = 100 nm, 15 and 75 µg/ml) for 3, 6, and 12 h and allowed to grow for an additional 36 h before being assessed for cell viability (MTT). Negative control is the culture medium without cells, meaning no viable cells; positive control is cells without AuNP, meaning 100% viability. Error bars: standard derivation of the mean.

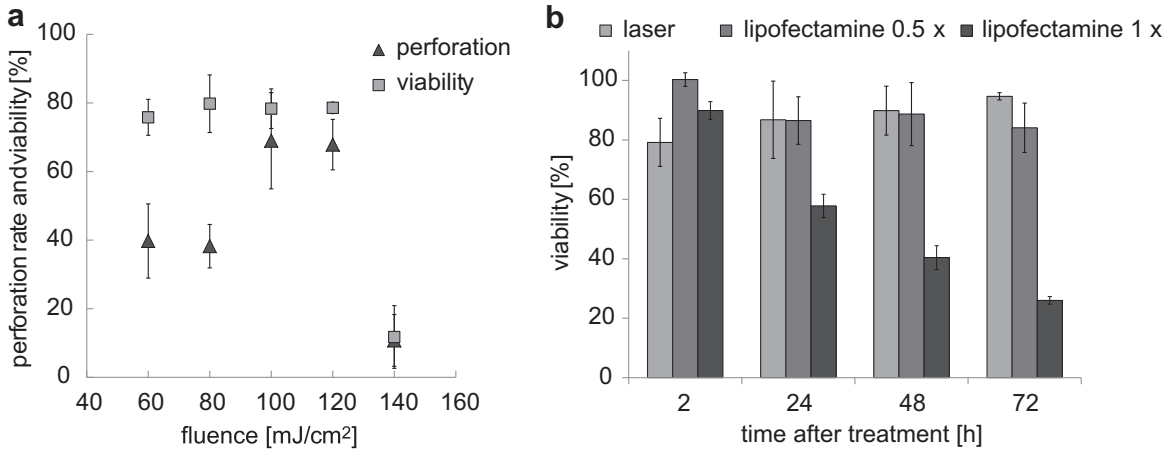

Fig. 2. Perforation efficiency and viability of the treated cells. (a) Perforation and transfection of human melanoma cells. Viability (squares) 2 h after the treatment and perforation rate of viable cells (triangles) depending on the laser fluence. (b) Viability of human melanoma cells 2–72 h after laser treatment or after lipofection (½× and 1× the recommended concentration) measured by MTT assay. Error bars: standard derivation; $n \geq 6$.

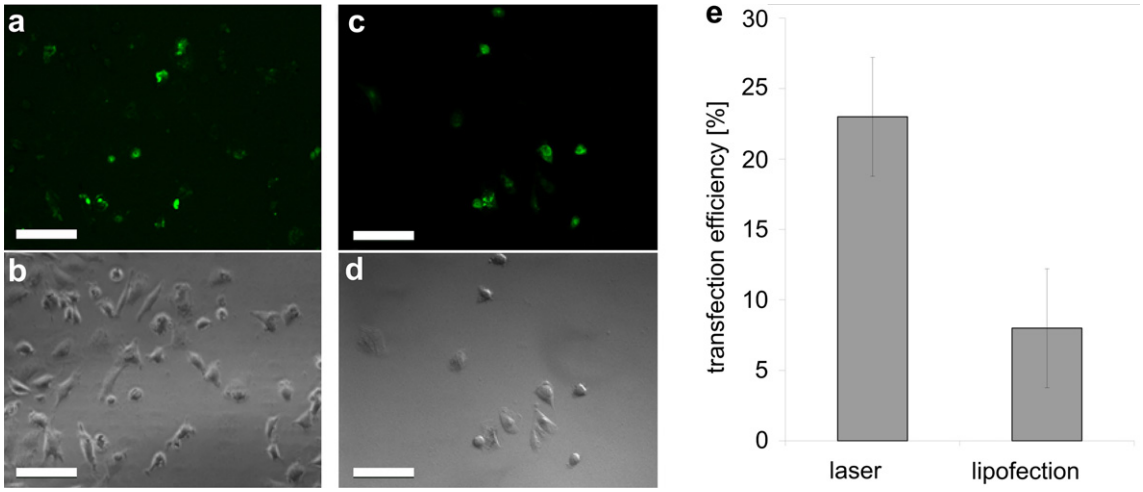

Fig. 3. Comparison of transfected cells with YFP-SMAD2 cDNA plasmid: fs laser plasmonic enhanced transfection and lipofection. Fluorescence (a) and phase contrast image (b) of cells transfected by plasmonic enhanced fs laser pulses; fluorescence (c) and differential interference contrast (DIC) image (d) of cells transfected by Lipofectamine. Scale bars: 100 μm. (e) Transfection efficiency of the laser based transfection method and lipofection. Error bars represent standard deviation; $n \geq 3$.

irradiation and that the irradiated internalized AuNP have no adverse effect on the cell growth. Additionally, the same experiment was performed with cells treated with two different quantities of lipofectamine (see Fig. 2b). The recommended volume of lipofectamine for efficient transfection (see methods) leads to a very poor viability of 90%, 58%, 41%, and 26% after 2 h, 24 h, 48 h, and 72 h, whereas half of this volume leads to a viability of 100%, 86%, 89%, and 84%, respectively. Hence, beside the very high optoporation efficiency, the laser based optoperforation approach offers much better long term viability in comparison to the optimized standard transfection method for this cell line as it does not rely on the use of toxic chemical agents.

3.4. Transfection by laser treatment in comparison to lipofection

The transfection of the WM278 melanoma cells was performed by perforation in presence of 50 μg/ml YFP-SMAD2 cDNA plasmid at a fluence of 100 mJ/cm^2 to study the transfection efficiency. The cells were incubated with 8 μg/ml AuNP (100 nm) during 4 h before the laser treatment; the transfection efficiency was measured 48 h after the treatment. The average transfection rate was 23% using the plasmonic enhanced fs laser based method (see Fig. 3a and e). The same cell line was transfected using Lipofectamine (lipofection) where 2 μg plasmid was mixed with 10 μl Lipofectamine 2000 reagent and added to the cells which were then incubated at 37 °C and 5% CO_2. Lipofection led to a transfection efficiency of 8% (see Fig. 3c and e) and a viability of the treated cells of 47% 2 h after the treatment compared to 52% for the laser treated cells.

3.5. Fragmentation study of gold nanoparticles

Although the general cytoxicity of bare AuNP was found to be negligible under working conditions, very small AuNP (nm range) produced by the laser irradiation may become toxic due to the risk of DNA intercalation, thereby blocking protein expression of the affected genes [30,31]. However, SEM images of nanoparticle

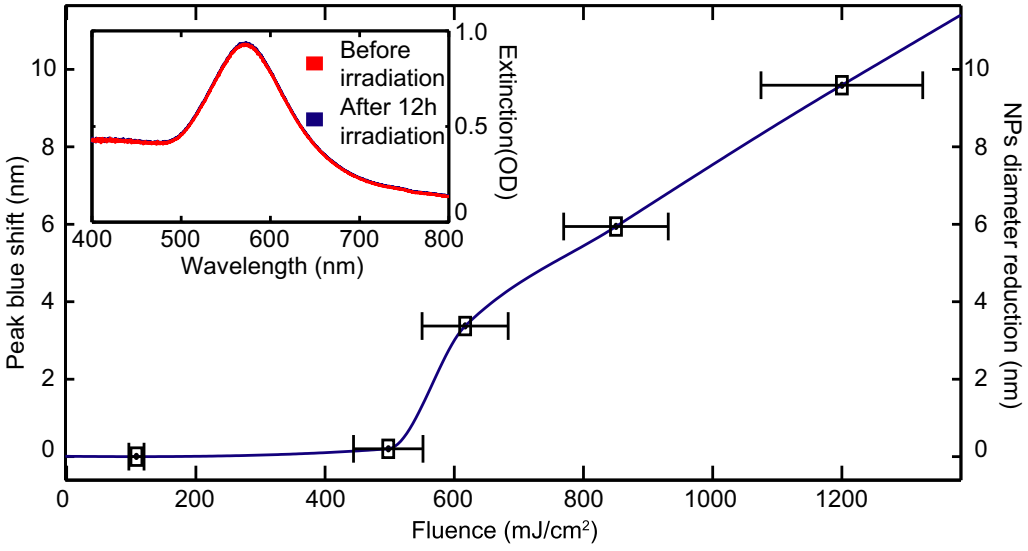

Fig. 4. Modification in the wavelength position of the extinction maximum of a solution of 100 nm AuNP following 12 h of irradiation from a 1 kHz 40fs 800 nm laser as a function of the incident laser fluence. Error bars represent twice the standard deviation. (The actual error bar for peak shift is ~0.3 nm, smaller than the point size). The right vertical axe shows the expected diameter change of a 100 nm as deduced from Mie theory. The inset compares the extinction spectrum before (blue) and after (red) 12 h irradiation for a fluence of 100 mJ/cm^2.

covered cells after the laser treatment did not significantly differ in terms of the number of AuNP on the cell membrane (91 ± 16), as well as the shape and size of the AuNP were not visibly changed after laser irradiation (see Fig. 1d). As seen in Fig. 4, this result is further confirmed by in-situ spectroscopic studies showing that a solution containing 50 μg/ml of spherical 100 nm diameter AuNP irradiated during 12 h with the laser parameters used for the transfection process experiences no significant modification ($\Delta\lambda < 0.03$ nm) of its extinction spectrum due to the irradiation. Such a modification would have been the fingerprint of a change in the particle size resulting from ablation or fragmentation [32]. Indeed, using Mie theory, it is possible to calculate the extinction spectrum for a nanosphere of a given diameter, and thus to relate a change in position of the extinction peak to a modification in the nanosphere diameter. Calculation reveals a change in the sphere diameter limited to 0.03 nm. Appreciable change in the extinction spectrum occurs for fluences 6 times higher than the one used in transfection experiments. Previous studies have also shown that non-thermal mechanisms may result in the ejection of some material layers from the nanoparticle to its environment following a laser irradiation [33], possibly leading to the formation of small AuNP. Results obtained although reveal that the concentration of such small AuNP is limited to <0.003 μg/ml for an initial 100 nm AuNP 8 μg/ml concentration, well below the ~1 μg/ml range reported to initiate cytotoxic effects [30]. All results hence show that the AuNP are not significantly affected and should not lead to the production of potentially toxic fragments produced during the laser treatment.

4. Conclusion

Overall, our results indicate that transfection of human cancer cells by using plasmonic enhanced fs laser pulses is a very promising method with a very high viability of the cells associated with an enhanced transfection efficiency compared to the classic lipofection approach. The setup allows a treatment of an area of 40 mm^2/min, so that a large number of adherent cells can be treated in an appropriate amount of time for biological or medical applications. In comparison, Chakraverty et al. reported that 10 min were required for the treatment of a 28 mm^2 area using carbon black nanoparticles to get similar results [27]. Especially, the cytotoxicity of the AuNP is very low (<1%), even though the cells internalize the particles. Additionally, there is only low heating of the AuNP and therefore no fragmentation to smaller particles that could intercalate into the DNA, so that even in vivo application for cells at the surface of the tissue would be possible. Furthermore, the comparison between the laser based plasmonic enhanced technique with commonly used lipofection shows a ~3-times higher transfection efficiency for the laser based method with equivalent cell viability. Additionally, the spatial selectivity is an important advantage for possible in vivo applications. Only laser exposed cells covered with nanoparticles are treated and a bioconjugation of those particles adds a cellular selectivity, leading to a treatment limited to the cells of interest, even in mixed culture or tissue. Therefore, the proposed method shows promises as an alternative transfection technology that could be adapted to therapeutic tools in the clinic.

Acknowledgement

The authors thank Le Fonds Québécois de la Recherche sur la Nature et les Technologies (FQRNT) and the German Research Foundation (DFG, BA 4121/1-1) for the financial support. The technical assistance by Yves Drolet and fruitful discussions with Sébastien Besner are also acknowledged.

References

[1] Walther W, Stein U. Viral vectors for gene transfer: a review of their use in the treatment of human diseases. Drugs 2000;60(2):249–71.
[2] Wong TK, Neumann E. Electric field mediated gene transfer. Biochem Biophys Res Commun 1982;107(2):584–7.
[3] Shigekawa K, Dower WJ. Electroporation of eukaryotes and prokaryotes: a general approach to the introduction of macromolecules into cells. Biotechniques 1988;6(8):742–51.
[4] Weaver J, Chizmadzhev Y. Theory of electroporation: a review. Bioelectrochem Bioenerg 1996;41:135–60.
[5] Graham FL, Smiley J, Russell WC, Nairn R. Characteristics of a human cell line transformed by DNA from human adenovirus type 5. J Gen Virol 1977;36(1):59–74.
[6] Wilson T, Papahadjopoulos D, Taber R. The introduction of poliovirus RNA into cells via lipid vesicles (liposomes). Cell 1979;17(1):77–84.
[7] Fraley R, Subramani S, Berg P, Papahadjopoulos D. Introduction of liposomeencapsulated SV40 DNA into cells. J Biol Chem 1980;255(21):10.431–5.
[8] Felgner PL, Tsai YJ, Sukhu L, Wheeler CJ, Manthorpe M, Marshall J, et al. Improved cationic lipid formulations for in vivo gene therapy. Ann N Y Acad Sci 1995;772:126–39.
[9] Stilwell JL, McCarty DM, Negishi A, Superfine R, Samulski RJ. Development and characterization of novel empty adenovirus capsids and their impact on cellular gene expression. J Virol 2003;77(23):12.881–5.
[10] Wold W, Doronin K, Toth K, Kuppuswamy M, Lichtenstein D, Tollefson A. Immune responses to adenoviruses: viral evasion mechanisms and their implications for the clinic. Curr Opin Immunol 1999;11:380–6.
[11] Menendez P, Bueno C, Wang L, Bhatia M. Human embryonic stem cells: potential tool for achieving immunotolerance? Stem Cell Rev 2005;1(2):151–8.
[12] Tirlapur UK, König K. Targeted transfection by femtosecond laser. Nature 2002;418(6895):290–1.
[13] Stevenson D, Agate B, Tsampoula X, Fischer P, Brown CTA, Sibbett W, et al. Femtosecond optical transfection of cells: viability and efficiency. Opt Express 2006;14(16):7125–33.
[14] Baumgart J, Bintig W, Ngezahayo A, Willenbrock S, Escobar HM, Ertmer W, et al. Quantified femtosecond laser based opto- perforation of living GFSHR-17 and MTH53 a cells. Opt Express 2008;16(5):3021–31.
[15] Kohli V, Acker JP, Elezzabi AY. Reversible permeabilization using high-intensity femtosecond laser pulses: applications to biopreservation. Biotechnol Bioeng 2005;92(7):889–99.
[16] Zeira E, Manevitch A, Manevitch Z, Kedar E, Gropp M, Daudi N, et al. Femtosecond laser: a new intradermal DNA delivery method for efficient, long-term gene expression and genetic immunization. FASEB J 2007;21(13):3522–33.
[17] Uchugonova A, König K, Bueckle R, Isemann A, Tempea G. Targeted transfection of stem cells with sub-20 femtosecond laser pulses. Opt Express 2008; 16(13):9357–64.
[18] Yao C, Rahmanzadeh R, Endl E, Zhang Z, Gerdes J, Hüttmann G. Elevation of plasma membrane permeability by laser irradiation of selectively bound nanoparticles. J Biomed Opt 2005;10(6):064.012.
[19] Pitsillides CM, Joe EK, Wei X, Anderson RR, Lin CP. Selective cell targeting with light-absorbing microparticles and nanoparticles. Biophys J 2003;84:4023–32.
[20] Lapotko D. Plasmonic nanoparticle-generated photothermal bubbles. Nanomedicine 2009;4(7):813–45.
[21] Pustovalov VK, Smetannikov AS, Zharov VP. Photothermal and accompanied phenomena of selective nanophotothermolysis with gold nanoparticles and laser pulses. Laser Phys Lett 2008;11:775–92.
[22] Vogel A, Noack J, Hüttman G, Paltauf G. Mechanisms of femtosecond laser nanosurgery of cells and tissues. Appl Phys B 2005;81:1015–47.
[23] Jachowski T, Bintig W, Eckert S, Baumgart J, Ngezahayo A, Heisterkamp A, et al. Mechanisms of femtosecond laser cellular optoporation. Proc SPIE; 2009:7373.
[24] Schomaker M, Baumgart J, Ngezahayo A, Bullerdiek J, Nolte I, Escobar H, et al. Ultrashort laser pulse cell manipulation using nano- and micro-materials. SPIE Proc; 2009:71920U.
[25] Houghton AN, Polsky D. Focus on melanoma. Cancer Cell 2002;2:275–8.
[26] Ho J, Chen H, Lebrun J-J. Novel dominant negative smad antagonists to TGFβ signaling. Cell Signal 2007;19:1565–74.
[27] Chakravarty P, Qian W, El-Sayed MA, Prausnitz MR. Delivery of molecules into cells using carbon nanoparticles activated by femtosecond laser pulses. Nat Nanotech 2010;5:607–11.
[28] Messinger BJ, von Raben KU, Chang KR, Barber PW. Local fields at the surface of noble-metal microspheres. Phys Rev B 1981;24:649.
[29] Hsu MY, Elder DE, Herlyn M. Melanoma: the wistar melanoma (wm) cell lines [Chapter 14]. In: Palsson JRWMaB, editor. Human cell culture, vol. 1. Kluwer Academic Publishers; 1999.
[30] Schaeublin NM, Braydich-Stolle LK, Schrand AM, Miller JM, Hutchison J, Schlager JJ, et al. Surface charge of gold nanoparticles mediates mechanism of toxicity. Nanoscale 2011;3:410–20.
[31] Skuridin SG, Dubinskaya VA, Rudoy VM, Dement'eva OV, Zakhidov ST, Marshak TL, et al. Effect of gold nanoparticles on DNA package in model systems. Doklady Biochem Biophys 2010;432:141–3.
[32] Besner S, Kabashin A, Meunier M. Fragmentation of colloidal nanoparticles by femtosecond laser-induced supercontinuum generation. Appl Phys Lett 2006; 89:233122.
[33] Plech A, Kotaidis V, Lorenc M, Boneberg J. Femtosecond laser near- field ablation from gold nanoparticles. Nat Phys Lett 2006;2:44–7.